DOI: https://doi.org/10.15407/pmach2025.03.072

UDC 621.3.013

COMPUTATIONAL AND EXPERIMENTAL STUDIES ON THE EFFICIENCY OF COMBINED ELECTROMAGNETIC SHIELDING OF THE MAGNETIC FIELD OF OVERHEAD POWER LINES

Ihor V. Bovdui

<u>ibovduj@gmail.com</u> ORCID: 0000-0003-3508-9781

Anatolii Pidhornyi Institute of Power Machines and Systems of NAS of Ukraine, 2/10, Komunalnykiv str., Kharkiv, 61046, Ukraine

To improve the efficiency of reducing the power frequency of the magnetic field generated by overhead power lines in residential buildings, experimental studies based on the results of 3D modeling when using a combined electromagnetic shield consisting of active and passive parts were conducted. The problem of designing a combined electromagnetic shield consisting of a robust active shielding system and an electromagnetic passive shield is solved on the basis of a multi-criteria antagonistic game between two players. The vector of game wins is calculated using the finite element calculation system COMSOL Multiphysics, and the game solution is calculated using particle multiswarm optimization algorithms. When designing combined electromagnetic shields, the coordinates of the spatial location of the shielding winding, currents and phases in the shielding windings of the robust active shielding system, as well as the geometric dimensions and thickness of the electromagnetic passive shield, were calculated. The results of experimental studies of the effectiveness of magnetic field shielding using 3D modeling for a residential building and a power line, when using combined electromagnetic shielding with active and passive parts, are given. For the first time, in order to increase the effectiveness of a combined electromagnetic shield, which consists of active and passive parts, and is designed to reduce the industrial frequency of the magnetic field created by overhead power lines in residential buildings, experimental studies using 3D modeling were conducted. According to the results of experimental studies, the effectiveness of shielding the output magnetic field was determined. It was found that the shielding coefficient of the electromagnetic passive shield is more than two units, and the effectiveness of the system with an active shield is more than four units, and for a system with a combined electromagnetic passive and active shield it is more than 10 units. The possibility of reducing the level of magnetic field induction in a residential building from power lines when using combined electromagnetic passive and active shielding to a level safe for the population is proven.

Keywords: magnetic field, 3D modeling of combined electromagnetic passive and active shielding, experimental studies.

Introduction

Prolonged exposure to sufficiently weak levels of the power-frequency magnetic field (MF) on the population, especially those living in residential buildings near power lines, leads to an increase in the level of oncological diseases [1–5]. In view of this, the search for methods and means of normalizing the level of the electromagnetic field in existing residential buildings near power lines, without evicting the population and decommissioning existing electrical networks, determines the economic and social feasibility of such research. In this regard, in world practice, methods for reducing the level of MF in existing residential buildings of this type to a safe level of MF for residents are being intensively developed [6–8].

In paper [9], the problem of synthesis of combined magnetic field shielding systems in a twodimensional setting is considered. This approach assumes consideration of the effectiveness of shielding in the central section of residential buildings. However, as further research has shown that, when shielding a magnetic field, it is necessary to reduce the level of magnetic field induction to a safe level along the entire length of a residential building. This makes it appropriate to formulate and solve the problem of synthesizing combined shields in a three-dimensional setting.

Aim of the paper is experimental study of the effectiveness of combined electromagnetic shielding, which includes shielding of MFs with active shielding systems and solid passive shields, in order to reduce the level of MFs generated by power lines in residential buildings.

This work is licensed under a Creative Commons Attribution 4.0 International License. © Ihor V. Bovdui, 2025

Problem statement

The geometric direct problem of quasimagnetostatics of a power-frequency magnetic field, which consists in calculating the magnetic field at any point in space for its given sources, is considered [10–11].

The theoretical basis for calculating the magnetic field generated by power lines in a homogeneous medium is the so-called quasistatic approximation of the system of Maxwell's equations

rot
$$H = j$$
; div $B = 0$; $B = \mu_0 H$,

where H i B are vectors of magnetic field strength and induction; j – vector of the extraneous current density, given by external sources and is different from zero only in a limited region occupied by conductors.

It is assumed that the given space, in which it is necessary to shield the output magnetic field using an active shielding system, is free from conductive and ferromagnetic media and does not contain magnetic field sources. Buildings and structures almost do not shield the power-frequency magnetic field.

Based on this, considering the area outside the current-carrying conductors, it can be assumed that the current density is zero (rot H = 0) and, thus, the potential field

$$\mathbf{H} = -\operatorname{grad} U_m; \quad \boldsymbol{H}_x = -\frac{\partial U_m}{\partial x}; \quad \boldsymbol{H}_y = -\frac{\partial U_m}{\partial y}; \quad \boldsymbol{H}_z = -\frac{\partial U_m}{\partial z},$$

where U_m is the scalar magnetic potential.

To simplify the mathematical model of high-voltage power lines, phase current-carrying conductors are often taken in the form of infinitely long and thin straight conductors, which allows the use of a two-dimensional magnetic field model that contains two spatial components along the 0X, 0Y axes and is independent of the Z coordinate along which the power line conductors are located.

However, in this case, the vertical sections of the controlled windings of the active shielding system create significant projections of the magnetic field vector along the Z coordinate, which makes it necessary to use a three-dimensional magnetic field model, which, in addition, also allows taking into account the component of the magnetic field vector along the 0Z coordinate, which is created by the power line wires due to their sagging between the power line supports.

When calculating the magnetic field for currents, the quasi-static approximation of the Maxwell's equation system is equivalent to the Biot-Savart law, which can be written in the form [10]

$$B(P) = \frac{\mu_0 I_m}{4\pi} \int_L \frac{[dl \times R]}{R^3},$$

where B(P) is the MF induction at the observation point P; dl is the circuit L element with current I_m ; R is the vector directed from the contour element dl to the observation point P.

The cube of the vector R magnitude is equal to

$$R = \sqrt{x_P^2 + y_P^2, +z^2}$$
; $R^3 = (x_P^2 + y_P^2, +z^2)^{3/2}$.

An approach to constructing a mathematical model of the magnetic field in a given space, based on the representation of power line current-carrying conductors, as well as windings of magnetic compensating elements in the form of a set of elementary sections of current-carrying conductors, is considered. This approach allows to calculate the magnetic field of current-carrying conductors of almost any shape, other than ideal straight lines, rectangles, etc., and also to take into account the sagging of current-carrying conductors of power lines.

Let's dwell on one of the approaches to constructing such a mathematical model of the magnetic field generated by a current-carrying conductor with a current *I* of a sufficiently complex design, based on the Biot-Savart-Laplace law.

We represent the considered current-carrying conductor in the form of elementary segments of a sufficiently small length and denote the coordinates of the middle of the segment as C_i . The vector of the magnetic field induction B, which was generated by this elementary segment located at point C_i , is established at point P with coordinates (x, y, z). Let's represent the elementary segment of the current-carrying conductor taking into account the direction of the current and the location of the segment itself in the orthogonal coordinate system in the form of orthogonal vectors a_x , a_y , a_z .

We define the components of the expansion of the vector of an elementary segment of a current-carrying conductor in an orthogonal coordinate system as the difference between the coordinates of the end and beginning of this segment in the following form:

$$(x_{i+1}-x_i), (y_{i+1}-y_i), (z_{i+1}-z_i),$$

and vector ΔL_i as the difference between the coordinates of the end and beginning of a given segment in this form:

$$\Delta L_i = (x_{i+1} - x_i)a_x + (y_{i+1} - y_i)a_y + (z_{i+1} - z_i)a_z.$$

Let's introduce the vector R_i , the beginning of which is located in the center of this elementary segment of the current-carrying conductor, and the end – at the point P(x, y, z), at which it is necessary to determine the vector of induction of the magnetic field created by the elementary segment of the current-carrying conductor, in the form

$$R_i = P - C_i = (x, y, z) - \left(\frac{x_{i+1} + x_i}{2}, \frac{y_{i+1} + y_i}{2}, \frac{z_{i+1} + z_i}{2}\right).$$

Then the vector B(x, y, z) of the total magnetic field induction at a given point P(x, y, z), generated by n elementary segments of a current-carrying conductor with current I, can be determined based on the Biot-Savart-Laplace law in the form [10]

$$B = \frac{\mu_0 I}{4\pi} \sum_{i=1}^n \frac{\Delta L_i \times R_i}{|R_i|^3} \,, \tag{1}$$

where μ_0 is the magnetic constant.

Cross product of vectors $\Delta L_i \times R_i$ is equal to the vector with the following components

$$\Delta L_i \times R_i = \left(\Delta L_{iy} R_{iz} - \Delta L_{iz} R_{iy} \right), \quad \left(\Delta L_{iz} R_{iy} - \Delta L_{ix} R_{iz} \right), \quad \left(\Delta L_{ix} R_{iy} - \Delta L_{iy} R_{ix} \right).$$

The notations ΔL_{ix} and R_{ix} and components of vector decomposition ΔL_i and R_i along the axis 0X, identical to the axes 0Y and 0Z, are introduced. The cube of the vector R_i magnitude is denoted as $|R_i|^3$, it is defined by

$$\left|R_{i}\right|^{3} = \left(\sqrt{R_{ix}^{2} + R_{iy}^{2} + R_{iz}^{2}}\right)^{3}.$$
 (2)

The solution of the geometric direct problem for power line wires – from the construction of a mathematical model of the output magnetic field generated by the power line – is considered. The position of the power line wires is known. We specify the currents in the power line wires in the form of sinusoidal dependences of instantaneous values depending on time, as well as the amplitude A_i and phase C_i of the power line wires of the power-frequency ω and the currents of the wires in the power line in complex form

$$I_i(t) = A_i \exp j(\omega t + \varphi_i).$$

Based on the obtained relation (2), the induction $B_0(P_i, I_0(t), t)$ of the output magnetic field at the point P_i , which is created by currents $I_l(t)$ in power lines current-carrying conductors l, can be calculated with the following formula:

$$B_0(P_i, I_0(t), t) = \sum_{l=1}^{L} B_{0l}(P_i, I_l(t)).$$
(3)

The vector $I_0(t)$ of the currents in the power lines is introduced. Its components are the currents $I_l(t)$ in power lines current-carrying conductors l,

$$I_0(t) = \left\{ I_l(t) \right\}.$$

It should be noted that when calculating the resulting magnetic field of the power line according to formula (3), for 3D modeling it is necessary to take into account the real sagging of the power line wires. In this case, the number of elementary sections of the power line conductors at the ends of the wire sections taken into account must be set with the necessary accuracy to calculate the induction of the resulting magnetic field generated by all power line wires at a given point in the shielding space.

Let's consider the solution of the forward problem for calculating the magnetic field generated by the compensating windings at the points of the shielding space. We specify the currently unknown coordinates of the location of the compensating windings of the active shielding system in the form of a vector X_a of the initial geometric values of the sizes of the compensating windings of the active protection, as well as the amplitude A_{ai} and the phase of the currents φ_{ai} in the compensating windings [10]. The currents in the wires of the compensating windings are found based on the complex form

$$I_{ai}(t) = A_{ai} \exp j(\omega t + \varphi_{wi}).$$

Then, for a given point P(x, y, z) of the shielding space, based on the Biot-Savart law, the elementary value of the magnetic field induction generated at a given point in space by an elementary section of the compensating winding wire can be calculated based on (1). Similarly, using (3), the induction $B_y(P_i, I_y(t), t)$ of the MF in the point P_i , which is created by the currents of the windings of the magnetic compensating elements at a point in time t, can be calculated by the following formula:

$$B_{y}(P_{i}, I_{y}(t), t) = \sum_{m=1}^{M} B_{ym}(P_{i}, I_{ym}(t), t),$$
(4)

here, the vector $I_y(t)$ of the currents in compensating windings, the components of which are the currents $I_l(t)$ in m windings is introduced

$$I_{y}(t) = \{I_{ym}(t)\}.$$

It should be noted that when calculating the resulting magnetic field generated by all wires of the compensating windings, according to formula (4), in 3D modeling, it is necessary to take into account not only the real dimensions of the horizontal parts of the compensating windings, but also the actual length of the compensating windings, since it is near the ends of the horizontal sections of the compensating windings that the greatest change in the level of induction of the magnetic field generated by the compensating windings is observed. Naturally, in 3D modeling, in formula (4), the vertical parts of the compensating windings should be taken into account, as they generate the main part of the magnetic field induction.

Then, according to the principle of superposition, the resulting vector $B(P_i, I_0(t), X_a, t)$ of the MF induction in the point P_i , which is generated by the currents $I_0(t)$ of the power lines wires $B_0(P_i, I_0(t), t)$ and compensating winding currents $B_y(P_i, X_a, t)$, is equal to the sum of the vectors

$$B(P_i, I_0(t), X_a, t) = B_0(P_i, I_0(t), t) + B_v(P_i, X_a, t).$$
(5)

Let's consider the solution of the forward problem for a continuous open passive shield. In this case, the instantaneous values of the vector $B(P_i, I_0(t), X_a, t)$ of the magnetic induction of the resulting magnetic field generated by power lines $B_0(P_i, I_0(t), t)$ and windings of the active shielding system $B_y(P_i, X_a, t)$ at any point of the shielding space, are considered given and are calculated by formula (5).

Let's dwell on the calculation of the magnetic field in the space in which the power lines current-carrying conductors, compensating windings and continuous electromagnetic shields of passive shielding are located. In this case, we will assume that the space in which the current-carrying conductors and the electromagnetic shield are located does not contain ferromagnetic and conductive elements, and therefore, the relative magnetic permeability of the external space will be set equal to unity, and the specific conductivity will be equal to zero.

Let's study steady processes when the currents in the wires are described by the dependencies for signals of a sinusoidal shape. Therefore, the distribution of the electromagnetic field in the system can be described in terms of complex amplitudes. The calculation of magnetic induction was performed in a quasi-stationary approximation, since the frequency of electric currents flowing through the current-carrying conductors is equal to the industrial one. The diameter of the power lines current-carrying conductors and compensating windings is much smaller than the distance between them, so they can be considered as "current threads". The distribution of the current density flowing through the current-carrying conductors will be represented as a sum of delta functions. Thus, the assumptions that were made when building a physically correct model of the process of electromagnetic shielding of the magnetic field of long current-carrying conductors have been formulated and justified.

Taking into account the assumptions made to find the distribution of the MF, we will use the law of the total current in the integral form, written in a quasi-stationary approximation in terms of complex amplitudes [6]

$$\oint_{l} H \, dl = \int_{S} \gamma \, E \, ds + \int_{S} J^{ext} \, ds$$

where H, E are complex amplitudes of the vectors, respectively, of the magnetic and electric field strengths; J^{ext} is the complex amplitude of the current density vector of current-carrying conductors; γ is the specific electrical conductivity; l is the contour covering the surface of integration s.

To describe an electromagnetic shield, it is necessary to specify its location relative to the current-carrying conductors, geometric dimensions, and magnetic permeability μ and specific electrical conductivity γ . The system of currents in power lines is described by the frequency ω and the current density distribution vector J^{ext} .

The numerical methods for calculating the magnetic field used for calculating electromagnetic shields is considered. The most widespread in the numerical study of the electromagnetic field, in particular, the quasi-stationary magnetic field, are the finite difference method, or the grid method, variational methods, the finite element method, and the method of integral equations [12–15]. The procedure for calculating the magnetic field is reduced to the composition and solution of a system of linear equations. The method of composition of this system, the form and dimension of its coefficient matrices for the listed numerical methods are quite different.

The finite difference method is based on the numerical solution of a differential equation, for example, an equation in a simple case, by replacing those derivatives of the unknown function included in it with expressions containing finite differences. Currently, the finite element method has become the most widespread for numerical solution. In this case, the computational domain is divided into a set of polygons of arbitrary shape, namely curvilinear in the general case, or triangular cells in the simple case. The function values at the grid nodes are initial, and an approximation by some function is introduced at the remaining points.

At the first stage, the initial parameters of the system are introduced: the geometric dimensions of the electromagnetic shield, its physical characteristics μ and γ , the magnitude and frequency of the currents in the current-carrying conductors. Next, the domain in which it is necessary to calculate the distribution of the MF is specified.

Based on this, the vector $B_p(P_i, X_p, t)$ can be calculated using the COMSOL Multiphysics software package. This is the vector of the instantaneous value of the magnetic field generated by the passive shield for a given vector of the instantaneous value of the induction of the output magnetic field $B(P_i, I_0(t), X_a, t)$, which is generated by the wires of the power line $B_0(P_i, I_0(t), t)$ and compensating windings $B_y(P_i, X_a, t)$ of the active shielding systems.

Such a mathematical model allows to calculate the distribution of magnetic induction of current-carrying conductors when using thin-walled electromagnetic shields consisting of several flat or U-shaped elements, and determine their shielding properties.

Using the COMSOL Multiphysics software package for a given vector X_a of the values of the geometric dimensions of the compensating windings, as well as currents A_{wi} and phases φ_{wi} in compensating windings, a given vector X_p of the geometric dimensions, thickness and material of the passive contour shield, it is possible to calculate the vector of the instantaneous value of the induction of the output magnetic field $B_R(P_i, X, \delta, t)$, which is generated by the wires of the power line $B_0(P_i, I_0(t), t)$, and compensating windings $B_y(P_i, X_a, t)$ of the active shielding system, as well as passive shielding $B_p(P_i, X_p, t)$, by the formula

$$B_{R}(P_{i}, I_{0}(t), X_{a}, X_{p}, t) = B_{0}(P_{i}, I_{0}(t), t) + B_{y}(P_{i}, X_{a}, t) + B_{p}(P_{i}, X_{p}, t).$$

Solution method

Let's consider the geometric inverse problem of magnetostatics, which consists in calculating the spatial location and parameters of magnetic field sources for generating a compensating magnetic field directed opposite to the initial magnetic field, in order to design a combined electromagnetic shield. In this case, the initial magnetic field is generated by the power line wires, and the compensating magnetic field is generated simultaneously by the compensating windings of the active shielding system and a solid passive shield.

Let's introduce the search parameter vector X, as a designing problem a combined shield whose components are the vector X_a of the values of geometric dimensions of compensating windings, currents A_{wi} and phases ϕ_{wi} in the compensating windings, as well as the vector X_p of the geometric dimensions, thickness and material of the passive contour shield [9]. Based on this, the designing problem a combined shield for given initial values of the search parameter vector X and the vector of uncertainty parameters δ is calculated as a value $B_R(P_i, X, \delta)$ of

the effective value of the instantaneous value of induction $B_R(P_i, X, \delta, t)$ of the resulting magnetic field at a point P_i of the shielding space using the finite element calculation system COMSOL Multiphysics, and the designing problem a passive shield is reduced to calculating the solution to the vector "game" [16–17]

$$B_R(X,\delta) = \langle B_R(X,\delta,P_i) \rangle. \tag{6}$$

Components of the vector $B_R(X, \delta, P_i)$, i.e. "game win", are effective values of the induction of the resulting magnetic field at all points P_i of space for shielding. In addition, in this vector "game" it is necessary to find the minimum of the "game wins" vector (6) by the vector X, and its maximum – by the vector X.

In this case, it is necessary to take into account the restrictions [12-15] on the search parameter vector X of the combined shield in the form of vector inequality and, possibly, vector equality.

It should be noted that the components of the vector "game" (6) are nonlinear functions of the search parameter vector and are calculated based on the finite element system COMSOL Multiphysics [12–15].

The method of solving the formulated problem is considered. Let's point out that for the correct solution of the multi-criteria optimization problem from Pareto-optimal solutions, in addition to the vector optimization criterion (6) and constraints, it is also necessary to have information about the binary ratios of the advantages of local solutions to each other [18]

max min max
$$B_R(P_i, X_j^*, \delta_j^*) < \max_{i=1,m} \min_{\mathbf{X}} \max_{\delta} B(P_i, X_k^*, \delta_k^*)$$
 (7)

Based on this, according to the relation (7), the solution X_j^* and δ_j^* are better than solutions X_k^* and δ_k^* . The physical meaning of the binary ratios of the advantages of local solutions to each other (7) is that solution X_j^* and δ_j^* provides a value of the resulting induction level lower than solution X_k^* and δ_k^* provides the maximum value of the induction in the entire space of searching for magnetic field shielding points with coordinates P_i precisely due to the binary ratios of the advantages of local solutions to each other (7). This happens because it provides a search for a solution that minimizes the maximum level of the resulting induction over the entire shielding space of the magnetic field. When solving the problem of scalar minimax optimization of the resulting induction at a specific point in the shielding space with coordinates Pi the induction value is minimized by the vector of parameters of the combined shielding system X, which must be found. To ensure the robustness of the combined shielding system, for each point of the shielding space, the resulting induction is maximized by the uncertainty vector δ .

Such approach allows to significantly reduce the set of possible optimal solutions of the initial multicriteria optimization problem and to facilitate the calculation process for the person making the decision regarding the choice of the optimal solution option from the area of Pareto-optimal solutions.

The problem of finding a local minimum at one point of a given space is, as a rule, multiextremal, the one that contains local minima and maxima, therefore, it is advisable to use stochastic multi-agent optimization algorithms to solve it. The algorithm for finding a set of Pareto-optimal solutions to multi-criteria nonlinear programming problems based on stochastic multi-agent optimization is considered. Nowadays, a significant number of particle swarm optimization algorithms have been developed – particle swarm optimization (PSO) algorithms, based on the idea of "collective intelligence of a particle swarm", such as the gbest PSO and lbest PSO algorithms [18–20].

The application of stochastic multi-agent optimization methods to solve multi-criteria problems causes certain difficulties, but this direction continues to develop intensively. To solve the original multi-criteria nonlinear programming problem with constraints, we will construct a stochastic multi-agent optimization algorithm based on a set of particle swarms, the number of which is equal to the number of components of the optimization criterion vector.

In the particle swarm optimization algorithm, the particle speeds change according to linear laws. In order to increase the speed of finding a global solution, special nonlinear stochastic multi-agent optimization algorithms have recently become widespread, in which the particle swarm motion is described by the following expressions [18–20]:

$$v_{ij}(t+1) = w_j v_{ij}(t) + c_{1j} r_{1j}(t) H(p_{1j} - \varepsilon_{1j}(t)) [y_{ij}(t) - x_{ij}(t)] + c_{2j} r_{2j}(t) H(p_{2j} - \varepsilon_{2j}(t)) [y_j^*(t) - x_{ij}(t)]$$

$$x_{ij}(t+1) = x_{ij}(t) + v_{ij}(t+1)$$

where $x_{ii}(t)$, $v_{ii}(t)$ are position and speed of particle i of the swarm j.

To take into account binary preference relations (7) when searching for solutions, special evolutionary algorithms for multi-criteria optimization were used [18, 19].

Experimental plant description

To conduct experimental studies to determine the effectiveness of shielding the magnetic field generated by overhead power lines, laboratory power line models have been developed for combined shields.

The appearance of a double-circuit power line model with a "barrel" arrangement of wires is shown in Fig. 1.

The appearance of the layout of a single-circuit power line with a triangular arrangement of wires is shown in Fig. 2. The current-carrying conductors of the power line layout are powered by an adjustable induction regulator.

The external appearance of two compensating windings of the active shielding system, made in the form of rectangular frames, with the winding wires located behind the ends of the surfaces, is shown in Fig. 3.

To power the compensating windings, two-channel power amplifiers, the appearance of which is shown in Fig. 4, are used. The power of each amplifier is up to 800 W per channel. In addition, the amplifier has the ability to be bridged, which provides a combined power of up to 1200 W per channel.



Fig. 1. Layout of a double-circuit power line with a "barrel" arrangement of wires



Fig. 3. Two compensating windings of the active shielding system



Fig. 2. Layout of a single-circuit power line with a triangular arrangement of wires



Fig. 4. Power amplifiers for powering compensating windings and measuring and recording devices

Fig. 5 shows the external view of the control system, consisting of sensors for measuring the magnetic field level; amplification units - forming input signals; phase inverter unit; controls for the system operator; measuring instruments for determining and setting the current level in the compensating windings; an oscilloscope for operational adjustment of control signals and recording current indicators at the operating point of the magnetic field sensors; a four-channel power amplifier up to 70 W per channel; a power supply unit for own needs and a power supply unit for the power amplifier.

For operational control and measurement of the resulting magnetic field in the middle of the shielding space, a three-coordinate magnetometer of the "TES 1394S triaxial ELF magnetic field meter" type, the appearance of which is shown in Fig. 6, is used.

The magnetometer measures the components of the magnetic field induction vector using three orthogonally arranged measuring coils, which are shown in Fig. 7. The axes of these measuring coils are or-

thogonal to each other and form an orthogonal coordinate system for measuring the magnetic field. Naturally, during the measurement, when positioning the device, the axes of these coils must be set parallel to the axes of the output magnetic field.



Fig. 5. Control system



Fig. 6. Three-coordinate magnetometer "TES 1394S"



Fig. 7. Location of the measuring coils of the magnetometer "TES 1394S"

Experimental studies of combined shields with solid passive shields

Let's consider experimental studies of a combined shield with a solid passive shield, in which the side surfaces of the latter are open, namely a U-shaped shield. A laboratory setup for this type of shield is shown in Fig. 8.

In the middle of the volume of the U-shaped passive shield, two magnetic field sensors are installed, which are used to implement two closed-loop control loops with two compensating windings of the active shielding system and feedback loops for the resulting magnetic field. The axes of the sensors are installed so as to measure the largest value of the magnetic field induction generated by the compensating winding of the corresponding compensating channel. Such installation of the axes of the magnetic field sensors allows to minimize the influence of the channels on each other during their joint operation.

In the middle of the volume of the passive shield, two additional magnetic field sensors, the axes of which are parallel



Fig. 8. Solid U-shaped passive shield

to the coordinate axes, are also installed. These sensors are used in a system for measuring the spatiotemporal characteristics of the resulting magnetic field. The measuring system is also used for operational adjustment of the control loops of the active shielding system of combined magnetic field shielding.

The shielding efficiency of the magnetic field generated by a double-circuit power line with a "barrel" arrangement of wires is considered. As a result of solving the geometric inverse problem of quasimagnetostatics, the coordinates of the location of two compensating windings of the active shielding system, as well as the currents and phases in them, were calculated. The distribution of the output field induction generated by a double-circuit power line with a "barrel" arrangement of wires is shown in Fig. 9.

Fig. 10 shows the distribution of the resulting field induction when only the U-shaped passive shield is used.

Fig. 11 shows the distribution of the resulting field induction when only the active shield is operating. The distribution of the resulting field induction during the operation of the combined shield is shown in Fig. 12.

The efficiency of the combined shield is 2–3 units. However, at the edges of the passive shield, the efficiency of shielding the output magnetic field is significantly reduced.

The efficiency of shielding the magnetic field generated by a single-circuit power line with a triangular arrangement of wires is considered. As a result of solving the geometric inverse problem of quasimagnetostatics, the coordinates of the location of two compensating windings of the active shielding system, as well as the currents and phases in them, were calculated.

The distribution of the induction of the output field generated by a single-circuit power line with a triangular arrangement of wires is shown in Fig. 13.

Fig. 14 shows the distribution of the resulting field induction when only the U-shaped passive shield is operating.

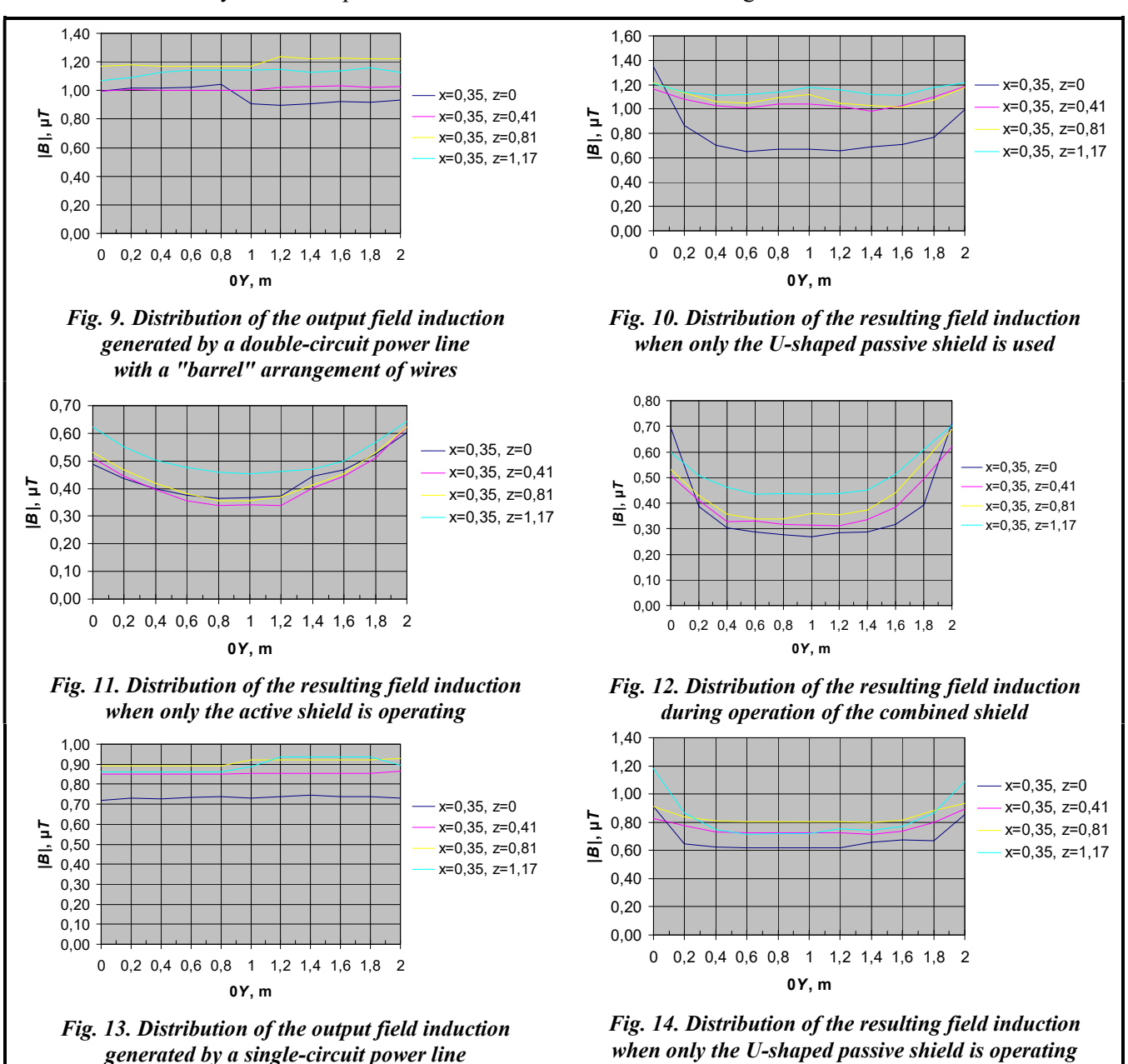
Fig. 15 shows the distribution of the resulting field induction when only the active shield is operating.

The distribution of the resulting field induction during the operation of the combined shield is shown in Fig. 16.

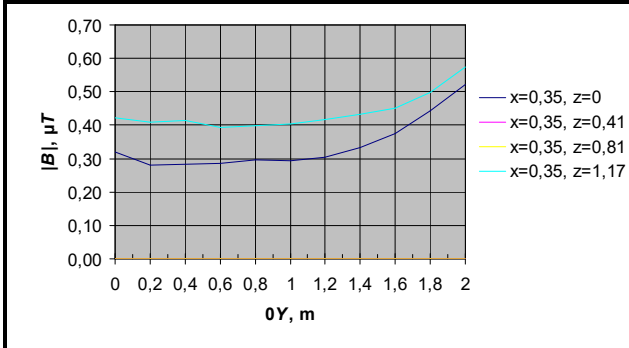
The efficiency of the combined shield is 2–3 units. However, at the edges of the passive shield, the efficiency of shielding the output magnetic field decreases significantly.

Experimental studies of a combined shield in which the side surfaces of the passive shield are covered with aluminum sheets are considered.

A laboratory shield setup with five shield surfaces is shown in Fig. 17.



with a triangular arrangement of wires



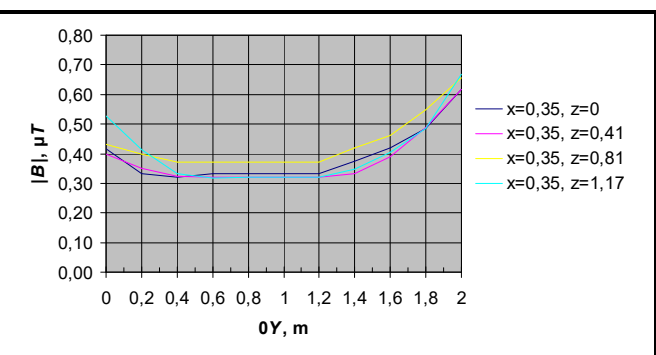


Fig. 15. Distribution of the resulting field induction when only the active shield is operating

Fig. 16. Distribution of the resulting field induction during the operation of the combined shield

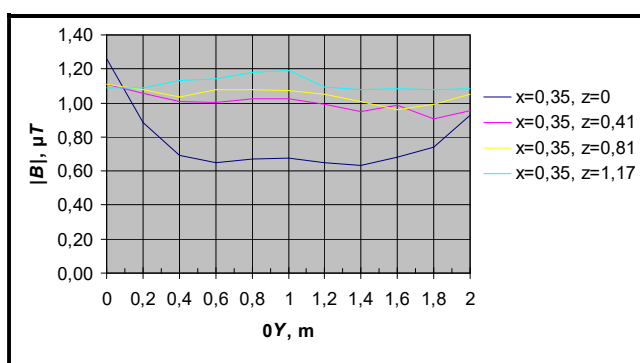
The efficiency of shielding the magnetic field generated by a double-circuit power line with a "barrel" arrangement of wires is considered. As a result of solving the geometric inverse problem of quasimagnetostatics, the coordinates of the location of two compensating windings of the active shielding system, as well as the currents and phases in them, were calculated. Naturally, the distribution of the induction of the output field generated by a double-circuit power line with a "barrel" arrangement of wires for this shield is the same as for a solid U-shaped shield, which is shown in Fig. 9.

Fig. 18 shows the distribution of the induction of the resulting field when only the passive shield is operating.

Fig. 19 shows the distribution of the resulting field induction when only the active shield is operating.



Fig. 17. A solid passive shield, in which the side surfaces of the passive shield are covered with aluminum sheets



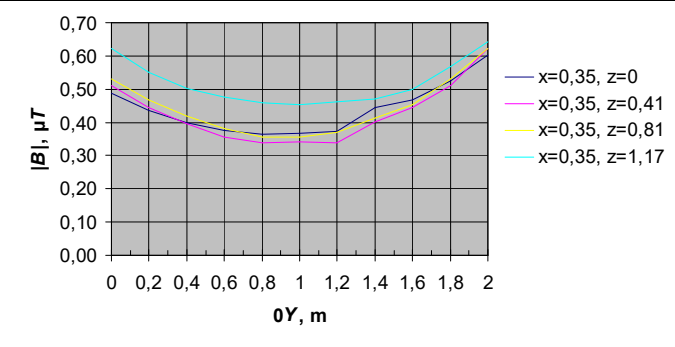


Fig. 18. Distribution of the resulting field induction when only the passive shield with five shield surfaces is used

|B|, μ7

0,60 0,50 0,40 0,30 0,20 0,00 0,00 0,00 0,20 0,40

Fig. 19. Distribution of the resulting field induction when only the active shield is operating

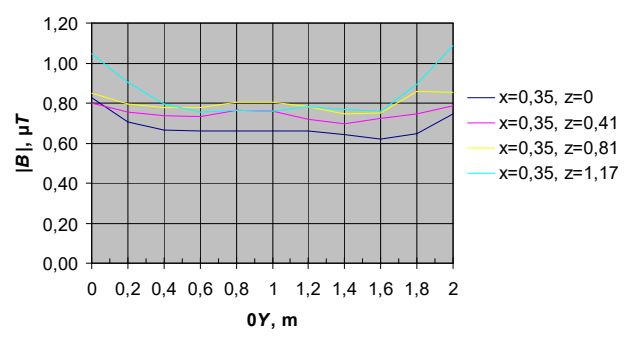


Fig. 20. Distribution of the resulting field induction during the operation of the combined shield

0Y, m

Fig. 21. Distribution of the resulting field induction when only the passive shield with five shield surfaces is used

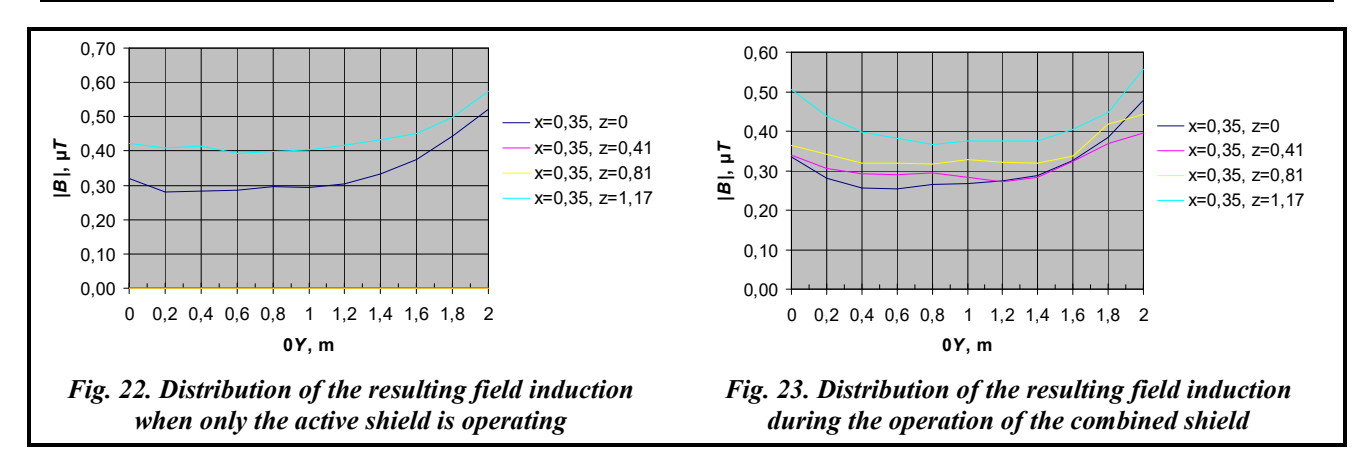


Fig. 20 shows the distribution of the resulting field induction during the operation of the combined shield. The shielding efficiency in the center of the shield with five surfaces is the same as in the case of a shield without side surfaces and is 2–3 units. However, in the areas at the edges of the passive shield, the shielding efficiency of the output magnetic field decreases significantly less than in the U-shaped shield, which is visible in Fig. 8. Such an increase in efficiency at the edges of the shield is due to the presence of side shielding surfaces.

The shielding efficiency of the magnetic field generated by a single-circuit power line with a triangular arrangement of wires is considered.

As a result of solving the geometric inverse problem of quasimagnetostatics, the coordinates of the location of two compensating windings of the active shielding system were calculated, as well as the currents and phases in these windings.

Naturally, the distribution of the induction of the output field generated by a single-circuit power line with a triangular arrangement of wires is the same for this shield as for the solid U-shaped shield, as shown in Fig. 10.

Fig. 21 shows the distribution of the resulting field induction when only the passive shield is operating. Fig. 22 shows the distribution of the resulting field induction when only the active shield is operating.

The distribution of the resulting field induction during the operation of the combined shield is shown in Fig. 23.

The shielding efficiency at the center of the shield with five surfaces is the same as for the shield without side surfaces and is 2–3 units. However, at the edges of the passive shield, the shielding efficiency of the output magnetic field decreases much less than that of the U-shaped shield, which is visible in Fig. 12. Such an increase in efficiency at the edges of the shield is due to the presence of side shielding surfaces.

Conclusions

- 1. The results of experimental studies of the effectiveness of combined electromagnetic shielding, including active and passive shielding using the solid shield and the magnetic field, which are based on 3D modeling, generated in residential buildings by single-circuit power lines with a triangular arrangement of wires, as well as for double-circuit power lines with a "barrel" arrangement of wires, are given.
- 2. The designing problem of combined shields is reduced to solving vector "games", in which the "game cost" vector is calculated using the COMSOL Multiphysics software package. The solutions of these vector "games" are calculated based on multiswarm optimization algorithms from a set of Pareto-optimal solutions taking into account binary ratios of the advantages of solutions of local criteria.
- 3. In the course of designing combined shields to reduce the level of MF generated by overhead power lines, the spatial coordinates of the two compensating windings, the currents and phases in these windings of the active shield, as well as the parameters of solid passive shields, U-shaped and with five surfaces, were calculated.
- 4. The main advantages of using combined electromagnetic shields consisting of active and solid passive parts are the reduction in the level of induction of the output MF in a much larger area of the shielding space compared to using only an active shield.
- 5. The practical application of combined electromagnetic shields allows to reduce the level of the magnetic field generated by the air of power lines inside residential buildings to a level that is safe for the population living near such power lines.

Gratitude

The author expresses his gratitude to the employees of the Department of Magnetism of Technical Objects of the Anatolii Pidhorny Institute of Power Machines and Systems of the NAS of Ukraine, Ph.D., Senior Researcher O. O. Tkachenko, engineers O. V. Sokol and O. P. Shevchenko for their assistance in the development and experimental testing of the combined electromagnetic shielding system.

References

- 1. Hardell, L. (2017). World Health Organization, radiofrequency radiation and health a hard nut to crack (Review). *International Journal of Oncology*, vol. 51, pp. 405–413. https://doi.org/10.3892/ijo.2017.4046.
- 2. Bray, F., Laversanne, M., Sung, H., Ferlay, J., Siegel, R. L., Soerjomataram, I., & Jemal, A. (2024). Global cancer statistics 2022: GLOBOCAN estimates of incidence and mortality worldwide for 36 cancers in 185 countries. *CA: a Cancer Journal for Clinicians*, vol. 74, iss. 3, pp. 229–263. https://doi.org/10.3322/caac.21834.
- 3. (2011). IARRC classifies radiofrequency electromagnetic fields as possibly carcinogenic to humans: Press release No. 2008. International Agency for Research on Cancer, 6 p. https://www.iarc.who.int/wp-content/uploads/2018/07/pr208 E.pdf.
- 4. (2013). Directive 2013/35/EU of the European Parliament and of the Council of 26 June 2013 on the minimum health and safety requirements regarding the exposure of workers to the risks arising from physical agents (electromagnetic fields). http://data.europa.eu/eli/dir/2013/35/oj.
- 5. (2002). IEEE standard for safety levels with respect to human exposure to electromagnetic fields, 0–3 kHz. In: IEEE Std C95.6-2002, pp. 1–64. https://doi.org/10.1109/IEEESTD.2002.94143.
- 6. Ghanim, T. H., Kamil, J. A., & Mutlaq, A. H. (2022). The influence of the mixed electric line poles on the distribution of magnetic field. *Indonesian Journal of Electrical Engineering and Informatics (IJEEI)*, vol. 10, no. 2, pp. 292–301. https://doi.org/10.52549/ijeei.v10i2.3572.
- 7. Canova, A. & Giaccone, L. (2018). Real-time optimization of active loops for the magnetic field minimization. *International Journal of Applied Electromagnetics and Mechanics*, vol. 56, pp. 97–106. https://doi.org/10.3233/jae-172286.
- 8. Canova, A. & Giaccone, L. (2017). High-performance magnetic shielding solution for extremely low frequency (ELF) sources. CIRED International Conference & Exhibition on Electricity Distribution, vol. 2017, iss. 1, pp. 686–690. https://doi.org/10.1049/oap-cired.2017.1029.
- 9. Canova, A., Giaccone, L., & Cirimele, V. (2019). Active and passive shield for aerial power lines. 25th International Conference on Electricity Distribution (3–6 June 2019, Madrid), paper 1096, 5 p. https://www.cired-repository.org/server/api/core/bitstreams/e782355b-54df-4be1-9964-3e614f13bf07/content.
- 10. Bravo-Rodríguez, J., del-Pino-López, J., & Cruz-Romero, P. A (2019). Survey on optimization techniques applied to magnetic field mitigation in power systems. *Energies*, vol. 12, iss. 7, pp. 1332–1332. https://doi.org/10.3390/en12071332.
- 11. Canova, A., del-Pino-Lopez, J. C., Giaccone, L., & Manca, M. (2015). Active shielding system for ELF magnetic fields. *IEEE Transactions on Magnetics*, vol. 51, iss. 3, pp. 1–4. https://doi.org/10.1109/tmag.2014.2354515.
- 12. Rusanov, A. V., Subotin, V. N., & Khoryev, O. M. (2022). Effect of 3D shape of pump-turbine runner blade on flow characteristics in turbine mode. *Journal of Mechanical Engineering Problemy Mashynobuduvannia*, vol. 25, no. 4, pp. 6–14. https://doi.org/10.15407/pmach2022.04.006.
- 13. Kostikov, A. O., Zevin, L. I., & Krol, H. H. (2022). The optimal correcting the power value of a nuclear power plant power unit reactor in the event of equipment failures. *Journal of Mechanical Engineering Problemy Mashynobuduvannia*, vol. 25, no. 3, pp. 40–45. https://doi.org/10.15407/pmach2022.03.040.
- 14. Maksymenko-Sheiko, K. V., Sheiko, T. I., & Lisin, D. O. (2022). Mathematical and computer modeling of the forms of multi-zone fuel elements with plates. *Journal of Mechanical Engineering Problemy Mashyno-buduvannia*, vol. 25, no. 4, pp. 31–38. https://doi.org/10.15407/pmach2022.04.032.
- 15. Hontarovskyi, P. P., Smetankina, N. V, & Ugrimov, S. V. (2022). Computational studies of the thermal stress state of multilayer glazing with electric heating. *Journal of Mechanical Engineering Problemy Mashynobuduvannia*, vol. 25, no. 2, pp. 14–21. https://doi.org/10.15407/pmach2022.02.014.
- Sushchenko, O., Averyanova, Yu., Ostroumov, I. V., Kuzmenko, N. S., Zaliskyi, M., Solomentsev, O., Kuznetsov, B., Nikitina, T., Havrylenko, O., Popov, A., Volosyuk, V., Shmatko, O., Ruzhentsev, N., Zhyla, S., Pavlikov, V., Dergachov, K., & Tserne, E. (2022). Algorithms for design of robust stabilization systems. In: Gervasi, O., Murgante, B., Hendrix, E. M. T., Taniar, D., & Apduhan, B. O. (eds). Computational Science and Its Applications ICCSA 2022. Lecture Notes in Computer Science. Springer, Cham, vol. 13375, pp. 198–213. https://doi.org/10.1007/978-3-031-10522-7 15.
- 17. Ummels, M. (2010). Stochastic Multiplayer Games Theory and Algorithms. Amsterdam: Amsterdam University Press, 174 p. https://doi.org/10.5117/9789085550402.

- 18. Ray, T. & Liew, K. M. (2002). A swarm metaphor for multiobjective design optimization. *Engineering Optimization*, vol. 34, no. 2, pp. 141–153. https://doi.org/10.1080/03052150210915.
- 19. Xiaohui, H., Eberhart, R. C., & Yuhui, S. (2003). Particle swarm with extended memory for multiobjective optimization. Proceedings of the 2003 IEEE Swarm Intelligence Symposium. SIS'03 (Cat. No. 03EX706). USA, Indianapolis, pp. 193–197. https://doi.org/10.1109/sis.2003.1202267.
- 20. Hashim, F. A., Hussain, K., Houssein, E. H., Mabrouk, M. S., & Al-Atabany, W. (2021). Archimedes optimization algorithm: a new metaheuristic algorithm for solving optimization problems. *Applied Intelligence*, vol. 51, pp. 1531–1551. https://doi.org/10.1007/s10489-020-01893-z.

Received 10 March 2025 Accepted 10 May 2025

Розрахунково-експериментальні дослідження ефективності комбінованого електромагнітного екранування магнітного поля повітряних ліній електропередачі

І. В. Бовдуй

Інститут енергетичних машин і систем ім. А. М. Підгорного НАН України 61046, Україна, м. Харків, вул. Комунальників, 2/10

Для підвищення ефективності зниження магнітного поля промислової частоти, створюваного повітряними лініями електропередачі в житлових будинках, проведено експериментальні дослідження за результатами 3D моделювання при застосуванні комбінованого електромагнітного екрану, який складається з активної та пасивної частин. Задача проєктування комбінованого електромагнітного екрану, який складається з робастної системи активного екранування та електромагнітного пасивного екрану, вирішується на основі багатокритеріальної антагоністичної гри двох гравців. Вектор виграшів гри розраховується з використанням системи кінцево-елементних обчислень COMSOL Multiphysics, а розв'язання гри – з застосуванням алгоритмів оптимізації мультироїв частинок. При проєктуванні комбінованих електромагнітних екранів розраховуються координати просторового розташування екрануючої обмотки, струми і фази в екрануючих обмотках робастної системи активного екранування, а також геометричні розміри і товщина електромагнітного пасивного екрану. Наведено результати експериментальних досліджень ефективності екранування магнітного поля з використанням 3D моделювання для житлового будинку та лінії електропередачі, при застосуванні комбінованого електромагнітного екранування, з активною й пасивною частинами. Вперше, з метою підвищення ефективності комбінованого електромагнітного екрану, який складається з активної та пасивної частин, та призначений для зниження магнітного поля промислової частоти, створюваного повітряними лініями електропередачі в житлових будинках, проведено експериментальні дослідження з використанням 3D моделювання. За результатами експериментальних досліджень, визначено ефективність екранування вихідного магнітного поля, встановлено, що коефіцієнт екранування електромагнітного пасивного екрана дорівнює більше двох одиниць, а ефективність системи з активним екраном – більше чотирьох одиниць, а для системи з комбінованим електромагнітним пасивним і активним екраном становить понад 10 одиниць. Доведена можливість зниження рівня індукції магнітного поля в житловому будинку від ліній електропередачі при використанні комбінованого електромагнітного пасивного й активного екранування до безпечного для населення рівня.

Ключові слова: повітряна лінія електропередачі, магнітне поле, 3D моделювання комбінованого електромагнітного пасивного та активного екранування, експериментальні дослідження.

Література

- 1. Hardell L. World Health Organization, radiofrequency radiation and health a hard nut to crack (Review). *International Journal of Oncology*. 2017. Vol. 51. P. 405–413. https://doi.org/10.3892/ijo.2017.4046.
- 2. Bray F., Laversanne M., Sung H., Ferlay J., Siegel R. L., Soerjomataram I., Jemal A. Global cancer statistics 2022: GLOBOCAN estimates of incidence and mortality worldwide for 36 cancers in 185 countries. *CA: a Cancer Journal for Clinicians*. 2024. Vol. 74. Iss. 3. P. 229–263. https://doi.org/10.3322/caac.21834.
- 3. IARRC classifies radiofrequency electromagnetic fields as possibly carcinogenic to humans: Press release No. 2008. International Agency for Research on Cancer. France, Lyon, 2011. 6 p. https://www.iarc.who.int/wp-content/uploads/2018/07/pr208 E.pdf.

- 4. Directive 2013/35/EU of the European Parliament and of the Council of 26 June 2013 on the minimum health and safety requirements regarding the exposure of workers to the risks arising from physical agents (electromagnetic fields). 2013. http://data.europa.eu/eli/dir/2013/35/oj.
- 5. IEEE standard for safety levels with respect to human exposure to electromagnetic fields, 0–3 kHz. In: IEEE Std C95.6-2002. 2002. P. 1–64. https://doi.org/10.1109/IEEESTD.2002.94143.
- 6. Ghanim T. H., Kamil J. A., Mutlaq A. H. The influence of the mixed electric line poles on the distribution of magnetic field. *Indonesian Journal of Electrical Engineering and Informatics (IJEEI)*. 2022. Vol. 10. No. 2. P. 292–301. https://doi.org/10.52549/ijeei.v10i2.3572.
- 7. Canova A., Giaccone L. Real-time optimization of active loops for the magnetic field minimization. *International Journal of Applied Electromagnetics and Mechanics*. 2018. Vol. 56. P. 97–106. https://doi.org/10.3233/jae-172286.
- 8. Canova A., Giaccone L. High-performance magnetic shielding solution for extremely low frequency (ELF) sources. CIRED International Conference & Exhibition on Electricity Distribution. 2017. Vol. 2017. Iss. 1. P. 686–690. https://doi.org/10.1049/oap-cired.2017.1029.
- 9. Canova A., Giaccone L., Cirimele V. Active and passive shield for aerial power lines. 25th International Conference on Electricity Distribution (3–6 June 2019, Madrid). 2019. Paper 1096. 5 p. https://www.cired-repository.org/server/api/core/bitstreams/e782355b-54df-4be1-9964-3e614f13bf07/content.
- 10. Bravo-Rodríguez J., del-Pino-López J., Cruz-Romero P. A Survey on optimization techniques applied to magnetic field mitigation in power systems. *Energies*. 2019. Vol. 12. Iss. 7. P. 1332–1332. https://doi.org/10.3390/en12071332.
- 11. Canova A., del-Pino-Lopez J. C., Giaccone L., Manca M. Active shielding system for ELF magnetic fields. *IEEE Transactions on Magnetics*. 2015. Vol. 51. Iss. 3. P. 1–4. https://doi.org/10.1109/tmag.2014.2354515.
- 12. Rusanov A. V., Subotin V. N., Khoryev O. M. Effect of 3D shape of pump-turbine runner blade on flow characteristics in turbine mode. *Journal of Mechanical Engineering Problemy Mashynobuduvannia*. 2022. Vol. 25. No. 4. P. 6–14. https://doi.org/10.15407/pmach2022.04.006.
- 13. Kostikov A. O., Zevin L. I., Krol H. H. The optimal correcting the power value of a nuclear power plant power unit reactor in the event of equipment failures. *Journal of Mechanical Engineering Problemy Mashynobuduvannia*. 2022. Vol. 25. No. 3. P. 40–45. https://doi.org/10.15407/pmach2022.03.040.
- 14. Maksymenko-Sheiko K. V., Sheiko T. I., Lisin D. O. Mathematical and computer modeling of the forms of multizone fuel elements with plates. *Journal of Mechanical Engineering Problemy Mashynobuduvannia*. 2022. Vol. 25. No. 4. P. 31–38. https://doi.org/10.15407/pmach2022.04.032.
- 15. Hontarovskyi P. P., Smetankina N. V, Ugrimov S. V. Computational studies of the thermal stress state of multi-layer glazing with electric heating. *Journal of Mechanical Engineering Problemy Mashynobuduvannia*. 2022. Vol. 25. No. 2. P. 14–21. https://doi.org/10.15407/pmach2022.02.014.
- Sushchenko O., Averyanova Yu., Ostroumov I. V., Kuzmenko N. S., Zaliskyi M., Solomentsev O., Kuznetsov B., Nikitina T., Havrylenko O., Popov A., Volosyuk V., Shmatko O., Ruzhentsev N., Zhyla S., Pavlikov V., Dergachov K., Tserne E. Algorithms for design of robust stabilization systems. In: Gervasi O., Murgante B., Hendrix E. M. T., Taniar D., Apduhan B. O. (eds). Computational Science and Its Applications ICCSA 2022. Lecture Notes in Computer Science. Springer, Cham, 2022. Vol. 13375. P. 198–213. https://doi.org/10.1007/978-3-031-10522-7 15.
- 17. Ummels M. Stochastic Multiplayer Games Theory and Algorithms. Amsterdam: Amsterdam University Press, 2010. 174 p. https://doi.org/10.5117/9789085550402.
- 18. Ray T., Liew K. M. A swarm metaphor for multiobjective design optimization. *Engineering Optimization*. 2002. Vol. 34. No. 2. P. 141–153. https://doi.org/10.1080/03052150210915.
- 19. Xiaohui H., Eberhart R. C., Yuhui S. Particle swarm with extended memory for multiobjective optimization. Proceedings of the 2003 IEEE Swarm Intelligence Symposium. SIS'03 (Cat. No. 03EX706). USA, Indianapolis, 2003. P. 193–197. https://doi.org/10.1109/sis.2003.1202267.
- 20. Hashim F. A., Hussain K., Houssein E. H., Mabrouk M. S., Al-Atabany W. Archimedes optimization algorithm: a new metaheuristic algorithm for solving optimization problems. *Applied Intelligence*. 2021. Vol. 51. P. 1531–1551. https://doi.org/10.1007/s10489-020-01893-z.